

This discussion paper is/has been under review for the journal The Cryosphere (TC).
Please refer to the corresponding final paper in TC if available.

A balanced water layer concept for subglacial hydrology in large scale ice sheet models

S. Goeller, M. Thoma, K. Grosfeld, and H. Miller

Alfred Wegener Institute for Polar and Marine Research, Am Alten Hafen 26,
27568 Bremerhaven, Germany

Received: 31 August 2012 – Accepted: 28 November 2012 – Published: 17 December 2012

Correspondence to: S. Goeller (sebastian.goeller@awi.de)

Published by Copernicus Publications on behalf of the European Geosciences Union.

TCD

6, 5225–5253, 2012

A balanced water layer concept

S. Goeller et al.

Title Page

Abstract

Introduction

Conclusions

References

Tables

Figures

◀

▶

◀

▶

Back

Close

Full Screen / Esc

Printer-friendly Version

Interactive Discussion



Abstract

There is currently no doubt about the existence of a wide-spread hydrological network under the Antarctic ice sheet, which lubricates the ice base and thus leads to increased ice velocities. Consequently, ice models should incorporate basal hydrology to obtain meaningful results for future ice dynamics and their contribution to global sea level rise. Here, we introduce the balanced water layer concept, covering two prominent subglacial hydrological features for ice sheet modeling on a continental scale: the evolution of subglacial lakes and balance water fluxes. We couple it to the thermo-mechanical ice-flow model RIMBAY and apply it to a synthetic model domain inspired by the Gamburtsev Mountains, Antarctica. In our experiments we demonstrate the dynamic generation of subglacial lakes and their impact on the velocity field of the overlying ice sheet, resulting in a negative ice mass balance. Furthermore, we introduce an elementary parametrization of the water flux–basal sliding coupling and reveal the predominance of the ice loss through the resulting ice streams against the stabilizing influence of less hydrologically active areas. We point out, that established balance flux schemes quantify these effects only partially as their ability to store subglacial water is lacking.

1 Introduction

Hundreds of subglacial lakes have been identified underneath the Antarctic ice sheet within the last decades (Siegert et al., 2005; Smith et al., 2009; Wright and Siegert, 2011). Observations also indicate interactions between lakes over several hundred kilometers (Wingham et al., 2006; Fricker et al., 2007, 2010; Fricker and Scambos, 2009) and thus reveal that these lakes are not isolated, but belong to a wide-spread subglacial hydrological network. Basal water lubricates the base of the ice sheet locally and hence leads to an acceleration of the overlying ice velocity. As a result, fast flowing ice streams evolve above subglacial water streams and the ice velocity increases over

TCD

6, 5225–5253, 2012

A balanced water layer concept

S. Goeller et al.

Title Page

Abstract

Introduction

Conclusions

References

Tables

Figures

◀

▶

◀

▶

Back

Close

Full Screen / Esc

Printer-friendly Version

Interactive Discussion



subglacial lakes (Bell et al., 2007). Increased ice velocities affect the mass balance of the Antarctic ice sheet and thus might have a considerable impact on global sea level rise. Consequently, it is an imperative necessity to incorporate basal hydrology into ice sheet modeling as it is considered to be one of the key parameters required to achieve more realistic results with respect to climate prediction (IPCC, 2007).

Despite the very low surface temperatures, large areas of the bed of the Antarctic ice sheet are at the pressure melting point, actively melting through the combined influence of the insulating ice cover and the geothermal heat flux into the base of the ice sheet. Model results show, that around 55% of the Antarctic ice sheet base could produce melt water while the rest of the ice sheet might be frozen to the bedrock (Pattyn, 2010).

For basal melt water transport we find, in principle, four possible water flow regimes: (a) flux through a system of linked cavities, which emerge by the ice flowing over bedrock bumps (Lliboutry, 1968), (b) flux through a water film between ice and bedrock (Weertman, 1972), or flux through channels which are either incised into (c) the ice base (Roethlisberger, 1972) or into (d) the bedrock (Nye, 1973).

In general, the basal water flux follows the gradient of the hydraulic potential which includes both the ice pressure and the bedrock elevation. However, the governing flow regime itself depends very much on the local geological properties at the ice base. They might range from solid bedrock, rough debris and till, to soft sediments. For the Antarctic ice sheet these very important basal conditions are only known from a very sparse number of boreholes. Thus, they are basically unknown for the majority of the Antarctic continent as the ice sheet base has been quite inaccessible for direct observations thus far.

Nevertheless, promising efforts have been made recently to gain mathematical descriptions of the water-pressure-dependent transition from one water flow regime to another (Schoof, 2010; Schoof et al., 2012; Hewitt, 2011; Hewitt et al., 2012). They are well implementable for the modeling of small mountain glaciers where high resolution data-sets of the order of hundreds of meters for ice thickness and bedrock elevation exist. However, for larger ice sheets or even continental scale modeling they

A balanced water layer concept

S. Goeller et al.

[Title Page](#)[Abstract](#)[Introduction](#)[Conclusions](#)[References](#)[Tables](#)[Figures](#)[◀](#)[▶](#)[◀](#)[▶](#)[Back](#)[Close](#)[Full Screen / Esc](#)[Printer-friendly Version](#)[Interactive Discussion](#)

A balanced water layer concept

S. Goeller et al.

[Title Page](#)[Abstract](#)[Introduction](#)[Conclusions](#)[References](#)[Tables](#)[Figures](#)[◀](#)[▶](#)[◀](#)[▶](#)[Back](#)[Close](#)[Full Screen / Esc](#)[Printer-friendly Version](#)[Interactive Discussion](#)

are inapplicable, since the available data basis is simply too coarse. Although numerous airborne campaigns in Antarctica (e.g. IceBridge, IceCap, IceGrav) make high-resolution bedrock digital elevation models available locally, typical elevation models for the whole Antarctic ice sheet provide the required geophysical data on a 5 km grid scale (Lythe et al., 2001; Le Brocq et al., 2010). Defining channelized water flux between adjacent grid cells at these scales would amount to single channels of large, unrealistic diameters. Even if a radio echo sounding coverage of Antarctica in the order of hundreds of meters would exist, the geological properties of the bedrock would be still unknown and the computational costs for the latter referred hydrological models would be huge.

Another well established method to trace the paths of subglacial melt water is the balance flux concept (Quinn et al., 1991; Budd and Warner, 1996; Tarboton, 1997; Le Brocq et al., 2006). This steady state approach assumes a basal hydraulic system in equilibrium and delivers the associated water flux for every grid cell without incorporating the latter different flow regimes. It is easy to implement, fast and well applicable to continental scale modeling (e.g. Pattyn, 2010). One disadvantage of this attempt to describe basal hydrology is the lacking mass conservation on realistic topographies: not all of the melt water produced inside the model domain reaches its margins but is partly lost inside the domain. In order to avoid that, hollows in the hydraulic potential have to be filled up. That again might result in the emergence of flat areas in the hydraulic potential and additional computational effort is necessary to conserve the flux over these flats. Furthermore, the balance flux concept provides no possibility for melt water to accumulate in hollows and to form subglacial lakes. This is of major importance for ice modeling since basal shear vanishes over lakes what crucially affects the ice sheet dynamics (Pattyn et al., 2004; Thoma et al., 2010, 2012).

To transfer the advantages of the balance flux concept and to overcome its weaknesses, we introduce the balanced water layer concept. This new approach is fully mass conservative on any topography without the necessity of any preceding modifications. For inclined regions of the hydraulic potential it yields the balance flux. In

addition, this concept allows water to accumulate in hollows of the hydraulic potential and hence to form subglacial lakes. Once lakes are filled to their maximum level, melt water generated upstream flows through the lakes to their discharge point and thus contributes to downstream flow.

5 In this paper we describe the new balanced water layer concept and couple it to the thermomechanical ice model RIMBAY (Thoma et al., 2010, 2012; Determann et al., 2012). The benefits of our new approach are demonstrated in the application to a synthetic model domain and the comparison with the original balance flux concept. We use an elementary parametrization of the sliding-law to clarify the complex interaction between ice dynamics and basal hydrology and their crucial impact on ice sheet dynamics and mass balance.

2 The ice model

15 In the present model study the three-dimensional thermomechanical finite differences ice-flow model RIMBAY is applied in shelfy-stream approximation (SSA) mode with a temperature-dependent viscosity. We choose a shelfy-stream-approach for grounded ice to incorporate shear stress coupling between adjacent grid cells, contrary to the conventional shallow-ice approximation (SIA) (e.g. Greve and Blatter, 2009). The computations for the ice dynamics are all performed on an Arakawa A-Grid (Arakawa and Lamb, 1977), treating model variables, e.g. bedrock elevation, ice thickness and velocity, as located at the grid center. Additionally, we introduce a basal water layer, which is situated between bedrock and ice base. The basal hydrology is directly coupled to the geometry of the ice model RIMBAY as the basal water layer can gain a certain thickness and thus lift the overlaying ice for this amount.

25 The boundary condition at the ice base for the calculation of the ice velocity \mathbf{v}_b is given by the sliding-law relationship $\boldsymbol{\tau}_b = \beta^2 \mathbf{v}_b$, where β^2 is defined as a Weertman

A balanced water layer concept

S. Goeller et al.

Title Page

Abstract

Introduction

Conclusions

References

Tables

Figures

◀

▶

◀

▶

Back

Close

Full Screen / Esc

Printer-friendly Version

Interactive Discussion



type sliding law and τ_b is the basal shear stress (e.g. Cuffey and Paterson, 2010).

$$\beta^2 = C^{\frac{1}{m}} |\tau_b|^{1-\frac{1}{m}} \quad (1)$$

$$\tau_b = -\rho_{\text{ice}} g H \nabla S \quad (2)$$

5 Here $m = 1/3$ is the sliding coefficient, C is the sliding rate, g is the gravitational acceleration, H is the ice thickness and ∇S is the ice surface gradient. Typical values for β^2 are the range of $\beta^2 = 0$ for a stress-free ice base (e.g. above subglacial lakes and for ice shelves) and $\beta^2 \approx 25\,000 \text{ Pa m}^{-1} \text{ a}$ (typical ice velocity of $v = 4 \text{ m a}^{-1}$ at a basal shear stress of $\tau = 100 \text{ kPa}$, Cuffey and Paterson, 2010). To describe the basal lubrication in dependency of the subglacial water flux ϕ with $[\phi] = \text{m}^2 \text{ s}^{-1}$ in a first-order approximation we define a flux-dependent sliding rate $C(\phi)$,

$$C(\phi) = C_0 \exp^{-m \frac{\phi}{\phi_0}} \quad (3)$$

15 with $C_0 = 10^7 \text{ Pa m}^{-1/3} \text{ s}^{1/3}$ and the reference flux ϕ_0 , scaling this correlation. Consequently, an increased flux ϕ implies a smaller sliding rate $C(\phi)$ and thus an enhanced slipperiness, which decreases β^2 to a possible minimum of zero. A reasonable reference flux ϕ_0 can be obtained by adapting it to observed ice surface velocities in specific Antarctic regions. In general, basal water fluxes for Antarctica elude direct observation but have been estimated for single discharge events of subglacial lakes to peak rates of $50 \text{ m}^3 \text{ s}^{-1}$ (Wingham et al., 2006).

20 The relation between deviatoric stress τ and strain rate $\dot{\epsilon}$ is given by Glen's flow law to $\dot{\epsilon} = A(T)\tau^n$ with $n = 3$ and a temperature-dependent rate factor $A(T)$. The evolution of the ice thickness H follows from the continuity equation

$$25 \frac{\partial H}{\partial t} = -\nabla(H\bar{v}) + A_S - M, \quad (4)$$

where \bar{v} is the vertically averaged ice velocity, A_S is the surface accumulation rate and M is the basal melt rate.

A balanced water layer concept

S. Goeller et al.

Title Page

Abstract

Introduction

Conclusions

References

Tables

Figures

◀

▶

◀

▶

Back

Close

Full Screen / Esc

Printer-friendly Version

Interactive Discussion



The ice temperature is calculated by solving the energy conservation equation and neglecting the horizontal diffusion. It is forced with the atmospheric temperature as a Dirichlet boundary condition at the surface and the geothermal heat flux as a Neumann boundary condition at the ice base. The basal melt rate M is given by (e.g. Pattyn, 2003)

$$M = \frac{1}{L\rho_{\text{ice}}} \left(k \frac{\partial T_b^*}{\partial z} + G \right), \quad (5)$$

where T_b^* is the basal ice temperature corrected for pressure melting, G is the geothermal heat flux, $L = 335 \text{ kJ kg}^{-1}$ is the specific latent heat of fusion and $k = 2.1 \text{ W m}^{-1} \text{ K}^{-1}$ the thermal conductivity for ice. We neglect the commonly used contribution of the frictional basal heating ($\tau_b \mathbf{v}_b / L\rho_{\text{ice}}$), since in the shelfy stream approximation the basal velocity \mathbf{v}_b corresponds to the high surface velocity and thus would dominate the influence of the other terms in Eq. (5) by orders of magnitude.

3 The balanced water layer concept

3.1 General formulation

The basal water generated by basal melting (Eq. 5) follows the gradient of the hydraulic potential P^t with $[P^t] = \text{m}$ (a.s.l. water equivalent) at the ice sheet base which takes into account the bedrock elevation B , the ice sheet pressure with local ice thickness H^t and the basal water layer thickness W^t .

$$P^t = B + W^t + H^t \frac{\rho_{\text{ice}}}{\rho_{\text{water}}} \quad (6)$$

After the ice thickness H^t and the melt rate M^t at time t were calculated, we obtain the local water layer thickness W^t by adding the melt water input $M^t \cdot \Delta t$ to the water layer

A balanced water layer concept

S. Goeller et al.

Title Page

Abstract

Introduction

Conclusions

References

Tables

Figures

◀

▶

◀

▶

Back

Close

Full Screen / Esc

Printer-friendly Version

Interactive Discussion



thickness W^{t-1} of the previous time step.

$$W^t = W^{t-1} + M^t \cdot \Delta t \quad (7)$$

Because H^t and W^t are time-dependent, the water layer thickness of the actual time step t might not be in equilibrium with respect to the hydraulic potential P^t anymore. Therefore we transport water in an iterative way along the gradient of the hydraulic potential until we find a stationary basal water distribution W^t satisfying (Eq. 6). This basic concept is applicable to all kind of ice models, whether they use a finite differences, finite elements or finite volumes discretization. Our ice model RIMBAY is based on finite differences. Consequently, in the next section we formulate the implementation of our hydrology model in finite differences, allowing a direct coupling of both models.

3.2 Implementation for finite differences

The potential $P_{i,j}^t$ for a grid cell (i, j) at time step t is composed of a constant part $P_{i,j}^{*t} = B_{i,j} + H_{i,j}^t \rho_{\text{ice}} / \rho_{\text{water}}$ and the adjustable water layer thickness $W_{i,j}^t$, which has to be balanced out with respect to the potential $P_{i,j}^t$. The iteration is all done for time step t , so we omit the time index for reasons of clarity.

$$P_{i,j} = P_{i,j}^* + W_{i,j} \quad (8)$$

The balanced water layer concept operates on an Arakawa C-grid (Arakawa and Lamb, 1977), which derives the gradients at the margins of the grid cells. Hence the gradients of the hydraulic potential $P_{i,j}$ are defined as

$$\frac{\partial P_{i,j}}{\partial x} = \frac{P_{i+1,j} - P_{i,j}}{\Delta x} \quad \text{and} \quad \frac{\partial P_{i,j}}{\partial y} = \frac{P_{i,j+1} - P_{i,j}}{\Delta y}. \quad (9)$$

The instantaneous transport of water between adjacent grid cells for one iterative step is expressed by $T_{i,j}^x$ and $T_{i,j}^y$, where the sign gives the direction and the product with the

A balanced water layer concept

S. Goeller et al.

Title Page

Abstract

Introduction

Conclusions

References

Tables

Figures

◀

▶

◀

▶

Back

Close

Full Screen / Esc

Printer-friendly Version

Interactive Discussion



grid size $\Delta x \Delta y$ the volume of the water transport (Fig. 1). To normalize all directional water transports *out* of a grid cell (i, j) we introduce the norm $N_{i,j}$ with

$$N_{i,j} = \max\left(\frac{\partial P_{i-1,j}}{\partial x}, 0\right) + \max\left(-\frac{\partial P_{i,j}}{\partial x}, 0\right) + \max\left(\frac{\partial P_{i,j-1}}{\partial y}, 0\right) + \max\left(-\frac{\partial P_{i,j}}{\partial y}, 0\right). \quad (10)$$

The differences of the potential between adjacent grid cells are defined as

$$\begin{aligned} \Delta_x P_{i,j} &= |P_{i+1,j} - P_{i,j}| \\ \Delta_y P_{i,j} &= |P_{i,j+1} - P_{i,j}|. \end{aligned} \quad (11)$$

So the water transports $T_{i,j}^x$ and $T_{i,j}^y$ can be calculated for all grid cell edges by

$$T_{i,j}^x = -\frac{\partial P_{i,j}}{\partial x} \begin{cases} \frac{\min(W_{i,j}, \varepsilon \Delta_x P_{i,j})}{N_{i,j}}, & \frac{\partial P_{i,j}}{\partial x} < 0 \\ \frac{\min(W_{i+1,j}, \varepsilon \Delta_x P_{i,j})}{N_{i+1,j}}, & \text{else} \end{cases}$$

$$T_{i,j}^y = -\frac{\partial P_{i,j}}{\partial y} \begin{cases} \frac{\min(W_{i,j}, \varepsilon \Delta_y P_{i,j})}{N_{i,j}}, & \frac{\partial P_{i,j}}{\partial y} < 0 \\ \frac{\min(W_{i,j+1}, \varepsilon \Delta_y P_{i,j})}{N_{i,j+1}}, & \text{else.} \end{cases} \quad (12)$$

with the convergence parameter $\varepsilon \in (0, 1)$. They are determined by the direction, the amount and the normalization of the water transfer. The sign of the hydraulic gradient (Eq. 9) gives the direction of the water transport in Eq. (12). The normalization is done by the ratio of the hydraulic gradient and $N_{i,j}$ of the water-contributing (upstream) grid

A balanced water layer concept

S. Goeller et al.

Title Page

Abstract

Introduction

Conclusions

References

Tables

Figures

◀

▶

◀

▶

Back

Close

Full Screen / Esc

Printer-friendly Version

Interactive Discussion



cell. To achieve convergence, we transport a water amount corresponding to a fraction ε of the differences of the potential (Eq. 11) only. If $\varepsilon\Delta_x P_{i,j}$ or $\varepsilon\Delta_y P_{i,j}$ exceeds the available amount of water $W_{i,j}$, at the maximum the latter can be transported.

Finally, we obtain the water layer for the next iteration step by

$$5 \quad W_{i,j}^{(\text{iter.}+1)} = W_{i,j}^{(\text{iter.})} + T_{i-1,j}^x - T_{i,j}^x + T_{i,j-1}^y - T_{i,j}^y, \quad (13)$$

and start again at Eq. (8), until we find the change of the water layer thickness for all n grid cells under a certain threshold $\Delta W^{(\text{threshold})}$

$$10 \quad \frac{1}{n} \sum_{i,j} \left| W_{i,j}^{(\text{iter.}+1)} - W_{i,j}^{(\text{iter.})} \right| \leq \Delta W^{(\text{threshold})}. \quad (14)$$

Here, the target precision of the basal water distribution rules the choice of $\Delta W^{(\text{threshold})}$, where a smaller value leads to a better levelness of subglacial lake surfaces but needs further iterations.

15 Closed lateral boundary conditions for the balanced water layer concept (e.g. at ice-nunatak interfaces) can be easily implemented by setting the water transport to zero at the respective grid cell edges. Open lateral boundaries do not require a special treatment. However, one can sum up all outward water transports at these margins to yield a water flux in order to force another coupled model, e.g. an ocean model at ice-ocean interfaces.

20 3.3 Scalar and vector water fluxes on C- and A-grids

The scalar volume flux Q with $[Q] = \text{m}^3 \text{s}^{-1}$ gives us the total water volume, which is horizontally transferred between adjacent grid cells within time step Δt . On a C-grid we consequently obtain $Q_{i,j}^x$ and $Q_{i,j}^y$, which are defined at the grid cell edges. We compute the volume flux by adding up all instantaneous water transports (Eq. 12) during the

A balanced water layer concept

S. Goeller et al.

Title Page

Abstract

Introduction

Conclusions

References

Tables

Figures

◀

▶

◀

▶

Back

Close

Full Screen / Esc

Printer-friendly Version

Interactive Discussion



above iteration

$$Q_{i,j}^x = \frac{\Delta x \Delta y}{\Delta t} \sum_{\text{iter.}} T_{i,j}^x, \quad Q_{i,j}^y = \frac{\Delta x \Delta y}{\Delta t} \sum_{\text{iter.}} T_{i,j}^y. \quad (15)$$

As the volume flux (Eq. 15) between two grid cells can be considered to be orthogonal to the grid cell edges, we can derive directly the vector flux ϕ with $[\phi] = \text{m}^2 \text{s}^{-1}$

$$\phi_{i,j}^x = \frac{Q_{i,j}^x}{\Delta y}, \quad \phi_{i,j}^y = \frac{Q_{i,j}^y}{\Delta x}. \quad (16)$$

It is fairly simple to couple the water flux calculated by the balanced water layer concept to an ice model running on a C-grid, because both water flux and ice velocities are determined at the edges of a grid cell.

Some more transformations are required, if one wants to derive a scalar and vector water flux at the grid cell center for a coupling with an A-grid ice model. First we approximate the total volume flux $Q_{i,j}^{(\text{out})}$ through a grid cell by the outflows $Q_{i,j}^x$ and $Q_{i,j}^y$ across the grid cell edges to

$$Q_{i,j}^{(\text{out})} = \max(-Q_{i-1,j}^x, 0) + \max(Q_{i,j}^x, 0) + \max(-Q_{i,j-1}^y, 0) + \max(Q_{i,j}^y, 0). \quad (17)$$

Then we determine the flux direction $\theta_{i,j}$ relative to the grid orientation by fitting a plane to the hydraulic potentials of the next four neighbour cells. According to Budd and Warner (1996) the vector flux $\phi_{i,j}$ at the center of a grid cell with side length $l = \Delta x = \Delta y$ is obtained by

$$\phi_{i,j} = \frac{Q_{i,j}^{(\text{out})}}{l(|\cos \theta_{i,j}| + |\sin \theta_{i,j}|)}. \quad (18)$$

A balanced water layer concept

S. Goeller et al.

Title Page

Abstract

Introduction

Conclusions

References

Tables

Figures

◀

▶

◀

▶

Back

Close

Full Screen / Esc

Printer-friendly Version

Interactive Discussion



The vector flux $\phi_{i,j}$ is the steady-state solution of the water thickness continuity equation

$$\frac{\partial W_{i,j}}{\partial t} = -\nabla \phi_{i,j} + M_{i,j} \stackrel{!}{=} 0 \quad (19)$$

5 with $\phi_{i,j} = W_{i,j} \vec{v}_{i,j}^{(\text{water})}$ and thus a balance flux.

4 Experiments and results

In the present study we use a rectangular model domain on the scale of $60 \times 200 \text{ km}^2$, a model resolution of 2 km and 21 terrain-following vertical ice layers. Our synthetic bedrock topography reflects typical characteristics of observations, e.g. in the Gamburtsev Mountains region in West Antarctica with peaks surmounting adjacent valleys up to 1 km on a horizontal kilometer scale (Bell et al., 2011). In our model domain the mountainous bedrock is reproduced by randomly distributed mountains with a linear increasing random amplitude up to 1 km from west to east (Fig. 2a). The northern, eastern and southern model domain margins are defined as free-slip closed boundaries. The western margin is defined as a fixed open boundary, where the ice sheet loses mass by calving, e.g. into an adjacent ocean. All experiments are carried out with the same bedrock topography to guarantee comparability. The model runs cover a timespan of 20 000 yr, so both ice dynamics and hydraulic system reach a steady state. The time step Δt is one year and always meets the Courant–Friedrich–Levy criteria $|\mathbf{v}| \Delta t / \Delta x \leq 1$. The surface temperature T_s is set to -10°C , the accumulation rate A_s is 0.5 ma^{-1} , and the geothermal heat flux G is 0.15 W m^{-2} all over the model domain. Compared to estimates for the Antarctic continent (Shapiro and Ritzwoller, 2004; Maule et al., 2005), we chose a geothermal heat flux in the upper range of the spectrum, which simply leads to a faster convergence of the basal hydraulic system in our model runs.

A balanced water layer concept

S. Goeller et al.

Title Page

Abstract

Introduction

Conclusions

References

Tables

Figures

◀

▶

◀

▶

Back

Close

Full Screen / Esc

Printer-friendly Version

Interactive Discussion



4.1 Initial state – control run

All experiments start with the same initial steady-state ice sheet (Fig. 2a), where the total accumulation balances the mass loss at the calving front at an ice volume of $17\,051\text{ km}^3$. The ice thickness of this parabolic ice sheet varies from 2298 m at the eastern margin to 266 m at the western ice sheet front, where the ice velocity increases up to 550 m a^{-1} . The variations of the ice velocity show clearly the influence of the mountainous bedrock (Fig. 2b). The melt rate (Eq. 5) is taken into account for the calculation of the ice thickness evolution (Eq. 4) and the vertical ice velocity. However, no subglacial hydrology model has been applied so far. Accordingly, there is no flux-sliding-coupling (Eq. 3) incorporated and $C(\phi) = C_0$ instead. The melt rate has a maximum of about 14 mm a^{-1} , where the ice thickness reaches its maximum and thus isolates the ice sheets base best from the surface temperature. It decreases considerably towards the ice sheet calving front (Fig. 2c).

4.2 Experiment A – subglacial lakes

Starting from the initial state, we apply the balanced water layer concept with $C(\phi) = C_0$. As a consequence melt water is able to accumulate in hollows of the hydraulic potential and starts to form subglacial lakes. We set the convergence parameters $\Delta W^{(\text{threshold})} = 10^{-10}\text{ m}$ and $\varepsilon = 0.5$, which is a good compromise between fast convergence and reasonable accuracy. The hydraulic system reaches a steady state after running the model for 20 000 yr, meaning all subglacial hollows are filled and the entire generated melt water of $0.1163\text{ km}^3\text{ a}^{-1}$ is leaving the model domain via its western margin. Grid cells, where the basal water layer thickness exceeds one meter, are defined as subglacial lakes. Above these lakes we assume a stress-free ice base and set $\beta^2 = 0$. In total we find 266 subglacial lakes covering 2253 km^2 (18.8 % of the model domain) with a water volume of 372 km^3 . The majority of the lakes is situated in the eastern part of the model domain, where the ice surface gradient is low and the bedrock elevation gradients are high. The surfaces of the lakes are inclined due to the basal

TCD

6, 5225–5253, 2012

A balanced water layer concept

S. Goeller et al.

Title Page

Abstract

Introduction

Conclusions

References

Tables

Figures

◀

▶

◀

▶

Back

Close

Full Screen / Esc

Printer-friendly Version

Interactive Discussion



pressure conditions resulting from the ice thickness gradients over the lakes (Fig. 3). This corresponds to observations in Antarctica, where lake surfaces reflect the ice surface slope with an amplification of factor nine. The largest lakes reach up to 100 km² extent and water depths up to 634 m (Fig. 4a). The ice velocity in *Exp. A* shows a clear evidence of variations in basal stresses, as there are many spots with an enhanced velocity in correlation with the location of subglacial lakes (Fig. 4b), and the total ice volume decreases to 16 484 km³, which will be discussed in Sect. 5.

4.3 Experiment B – flux-sliding coupling

In a second experiment we extend *Exp. A* by coupling the basal water flux (Eq. 18) to the basal sliding rate (Eq. 3). We set the reference flux to $\phi_0 = 10^4 \text{ m}^2 \text{ a}^{-1}$, which is just an example to illustrate the flux-sliding interaction. The generated melt water amounts to $0.1159 \text{ km}^3 \text{ a}^{-1}$. Figure 5a shows the basal balance water flux with a maximum of $13564 \text{ m}^2 \text{ a}^{-1}$, forming a branchy stream system. All the melt water from upstream areas flows through plenty of subglacial lakes towards the western model margin. The feedback of the flux-sliding coupling to the distribution and water volume of the subglacial lakes is minimal. In comparison to *Exp. A* their total volume diminishes by only 1.1 % to 368 km^3 . As a consequence of the flux-sliding coupling ice streams evolve above the very focussed subglacial water streams. They are about 4 km wide and move about 20 ma^{-1} ($\approx 40\%$) faster than the adjacent ice (Fig. 5b). Arteries of increased ice velocities reach also far upstream into the ice sheet where still velocity differences to *Exp. A* of up to 5 ma^{-1} ($\approx 25\%$) can be seen, locally. The ice velocity reaches its maximum with 558 ma^{-1} at the western ice sheet front. Consequently, the total ice volume diminishes to $16\,111 \text{ km}^3$.

4.4 Budd and Warner A and B

We perform two more benchmark experiments, where we apply the Budd and Warner (1996) balance flux scheme with the same flux-sliding coupling as in *Exp. B*. In *Budd*

A balanced water layer concept

S. Goeller et al.

Title Page

Abstract

Introduction

Conclusions

References

Tables

Figures

◀

▶

◀

▶

Back

Close

Full Screen / Esc

Printer-friendly Version

Interactive Discussion



and Warner *A* (*BWA*) we only use the hydraulic potential (Eq. 6) with $W = 0$ for the calculation of the balance flux. In *Budd and Warner B* (*BWB*) we fill all hollows in the hydraulic potential before the latter calculation. Thereby we do not only set local minima to the value of their lowest neighbor. Instead, we use a more complex algorithm to ensure, that hollows with more than one minimum are filled too. After that we slightly taper the resulting flats in the direction of their previously identified discharge point to guarantee flux conservation. As a result in *BWB* the entire generated melt water of $0.1156 \text{ km}^3 \text{ a}^{-1}$ is leaving the model domain at the calving front from the beginning. In *BWA* only the constant water flux of $0.0305 \text{ km}^3 \text{ a}^{-1}$ crosses this model margin, and the significantly bigger part of $0.0857 \text{ km}^3 \text{ a}^{-1}$ (74 % of the generated melt water in the amount of $0.1162 \text{ km}^3 \text{ a}^{-1}$) is lost in hollows of the hydraulic potential. Since the Budd and Warner scheme does not provide the accumulation of water in subglacial hollows, in both experiments no subglacial lakes emerge. The ice volume diminishes as a consequence of the flux-sliding coupling to $16\,983 \text{ km}^3$ in *BWA* and to $16\,666 \text{ km}^3$ in *BWB*.

5 Discussion

The comparison of the subglacial water balance for all experiments is shown in Fig. 6a. In *BWA* the majority of the generated melt water is lost inside the model domain. This confirms the necessity of the preceding modification of the hydraulic potential (described in Sect. 4.4) in *BWB* to obtain reasonable results with that method, which means an additional computational effort. This extra effort is not required for the balance water layer concept, which is water volume conserving on any hydraulic potential. Additionally, the fluxes into hollows of the hydraulic potential and over the model margin show a time-dependent behaviour in *Exp. A and B*. Both start with the same values as *BWA*. Then the flux into hollows of the hydraulic potential decreases as these slowly fill up. Simultaneously the flux over the model margin increases. The small steps in the time series of the fluxes indicate the time, when single hollows are filled and thus

A balanced water layer concept

S. Goeller et al.

Title Page

Abstract

Introduction

Conclusions

References

Tables

Figures

◀

▶

◀

▶

Back

Close

Full Screen / Esc

Printer-friendly Version

Interactive Discussion



the entire melt water, produced in their upstream catchment area, starts contributing to downstream areas and the flux over the model margin. Once all hollows are filled, the entire generated melt water is transported through them and contributes to the flux over the model margin as in *BWB*. So the balanced water layer concept is able to describe the transitional behaviour of the hydraulic system between *BWA* and *BWB*.

The differences of the absolute ice velocity between the experiments and the initial state reveal the influence of the basal hydraulic system on ice dynamics and mass balance. *Exp. A* indicates, that ice velocities above subglacial lakes are increased, while downstream of the lakes the velocity decreases again (Fig. 7a). This effect is consistent with observations of the surface velocity field based on radar interferometry, e.g. for Lake Vostok by Kwok et al. (2000), and could be reproduced by models for a single lake (Pattyn et al., 2004; Thoma et al., 2010, 2012). Although the velocity increase of the ice in *Exp. A* is only a local phenomenon above subglacial lakes, they do have an impact on the mass balance of the entire ice sheet. Figure 6b shows the temporal development of the total ice and lake volume for the different experiments (Summary in Table 1). Compared to the initial state, we find for *Exp. A* an ice loss of 567 km^3 (-3.3%). Taking into consideration the stored subglacial water volume of 372 km^3 , which replaced the corresponding ice volume, there is still an overall volume ($V_{\text{ice}} + V_{\text{water}}$) loss of 195 km^3 (-1.1%). In comparison to the direct mass loss caused by basal melting of $0.1163 \text{ km}^3 \text{ a}^{-1}$, the indirect contribution of the accumulated basal water to the mass balance of the ice sheet is large.

Due to the flux-sliding coupling the ice velocity field in *Exp. B* shows also the imprint of the basal water fluxes (Fig. 7b). Ice streams drain mass from the central areas and thus cause a thinning and flattening of the ice sheet. That again results in a lower basal shear stress (Eq. 2), which is driven by the ice surface gradient. Consequently, less hydrologically active areas beside the ice streams show significantly lower ice velocities and therefore contribute to a stabilization of the ice sheet. Nevertheless, the mass balance of *Exp. B* compared to the initial state is negative, since the ice volume is reduced by 940 km^3 (-5.5%). The overall volume loss amounts to 572 km^3 (-3.4%).

A balanced water layer concept

S. Goeller et al.

Title Page

Abstract

Introduction

Conclusions

References

Tables

Figures

◀

▶

◀

▶

Back

Close

Full Screen / Esc

Printer-friendly Version

Interactive Discussion



In *BWA* only 26 % of the melt water reaches the model margin, thus the effect of the flux-sliding coupling is relatively small and the ice volume solely decreases by 68 km^3 (-0.4%). The ice velocity field in *BWB* (Fig. 7c) shows the influence of the basal water fluxes just as *Exp. B*. However, since this approach is not capable of storing melt water, the impact of the subglacial lakes on ice dynamics is missing. As a consequence the ice volume diminishes for the amount of 385 km^3 (-2.3%) only.

In subsequent studies the potential of the new concept to analyse the dynamic evolution and interaction of lakes and subglacial water streams would allow one to estimate the impact of changed forcing parameters of the ice model on the basal hydrological system. So climate changes, e.g. variations of the accumulation rate and surface temperature, could affect the ice thickness and thus the hydraulic potential at the ice base, which could redirect subglacial water streams at a continental scale (Wright et al., 2008) or cause subglacial outburst floodings (Wingham et al., 2006).

6 Conclusion

The introduced balanced water layer concept for subglacial hydrology takes a different approach than existing balance flux schemes (Quinn et al., 1991; Budd and Warner, 1996; Tarboton, 1997). It yields a mass conserving balance flux on any topography and is able to accumulate water in subglacial hollows, where subglacial lakes can develop. These outcomes can be coupled to any ice model, operating in shallow-ice, shallow-shelf or higher-order approximation on numerical Arakawa A- or C-grids. The water layer thickness modifies the geometry by lifting the ice base, while water fluxes can be parameterized to increase the basal ice velocities. Above subglacial lakes the basal shear stress of the ice vanishes completely. In contrast to high-resolution water flow concepts (Hewitt et al., 2012; Schoof et al., 2012) our new approach is applicable to continental scale modeling, where only data sets of coarse resolution exist and computation time is an issue. The provided dynamic generation of subglacial lakes and the self-organization of subglacial water drainage systems combined with a flux-friction

A balanced water layer concept

S. Goeller et al.

Title Page

Abstract

Introduction

Conclusions

References

Tables

Figures

◀

▶

◀

▶

Back

Close

Full Screen / Esc

Printer-friendly Version

Interactive Discussion



coupling improve the modeled dynamics of glacial systems. Therefore, our concept has the potential for better prediction of the mass export of large ice sheets under the influence of climate warming, and thus their contribution to future global sea level rise.

Acknowledgements. This work was funded by the Helmholtz Climate Initiative REKLIM (Regional Climate Change), a joint research project of the Helmholtz Association of German research centres (HGF), and through the DFG research grant MA3347/2-1. The authors wish to thank Christoph Mayer for his collaboration in this project, Angelika Humbert for fruitful discussions as well as Conor Purcell for proof reading.

References

- 10 Arakawa, A. and Lamb, V. R.: Methods of Computational Physics, Vol. 17, Academic Press, 1977. 5229, 5232
- Bell, R. E., Studinger, M., Shuman, C. A., Fahnestock, M. A., and Joughin, I.: Large subglacial lakes in East Antarctica at the onset of fast-flowing ice streams, *Nature*, 445, 904–907, 2007. 5227
- 15 Bell, R. E., Ferraccioli, F., Creyts, T. T., Braaten, D., Corr, H., Das, I., Damaske, D., Frearson, N., Jordan, T., Rose, K., Studinger, M., and Wolovick, M.: Widespread persistent thickening of the East Antarctic ice sheet by freezing from the base, *Science*, 331, 1592–1595, 2011. 5236, 5249
- Budd, W. F. and Warner, R. C.: A computer scheme for rapid calculations of balance-flux distributions, *Ann. Glaciol.*, 23, 21–27, 1996. 5228, 5235, 5238, 5241
- 20 Cuffey, K. M. and Paterson, W. S. B.: *The Physics of Glaciers*, 4 edn., Elsevier, Amsterdam, 2010. 5230
- Determann, J., Thoma, M., Grosfeld, K., and Massmann, S.: Impact of ice-shelf basal melting on inland ice-sheet thickness: a model study, *Ann. Glaciol.*, 53, 129–135, 2012. 5229
- 25 Fricker, H. A. and Scambos, T.: Connected subglacial lake activity on lower Mercer and Whillans ice streams, West Antarctica, 2003–2008, *J. Glaciol.*, 55, 303–315, 2009. 5226
- Fricker, H. A., Scambos, T., Bindschadler, R., and Padman, L.: An active subglacial water system in west Antarctica mapped from space, *Science*, 315, 1544–1548, 2007. 5226

A balanced water layer concept

S. Goeller et al.

Title Page

Abstract

Introduction

Conclusions

References

Tables

Figures

◀

▶

◀

▶

Back

Close

Full Screen / Esc

Printer-friendly Version

Interactive Discussion



A balanced water layer concept

S. Goeller et al.

[Title Page](#)[Abstract](#)[Introduction](#)[Conclusions](#)[References](#)[Tables](#)[Figures](#)[◀](#)[▶](#)[◀](#)[▶](#)[Back](#)[Close](#)[Full Screen / Esc](#)[Printer-friendly Version](#)[Interactive Discussion](#)

- Fricker, H. A., Scambos, T., Carter, S., Davis, C., Haran, T., and Joughin, I.: Synthesizing multiple remote-sensing techniques for subglacial hydrologic mapping: application to a lake system beneath MacAyeal Ice Stream, West Antarctica, *J. Glaciol.*, 56, 187–199, 2010. 5226
- Greve, R. and Blatter, H.: *Dynamics of Ice Sheets and Glaciers*, Springer Verlag, 2009. 5229
- 5 Hewitt, I. J.: Modelling distributed and channelized subglacial drainage: the spacing of channels, *J. Glaciol.*, 57, 302–314, 2011. 5227
- Hewitt, I. J., Schoof, C., and Werder, M. A.: Flotation and free surface flow in a model for subglacial drainage. Part 2. Channel flow, *J. Fluid Mech.*, 702, 157–187, 2012. 5227, 5241
- 10 IPCC: The physical science basis, contribution of working group I to the fourth assessment report of the intergovernmental panel on climate change, in: *Climate Change 2007*, edited by: Solomon, S., Qin, D., Manning, M., Chen, Z., Marquis, M., Averyt, K. B., Tignor, M., and Miller, H. L., Cambridge University Press, Cambridge, United Kingdom and New York, NY, USA, 1009 pp., 2007. 5227
- Kwok, R., Siegert, M. J., and Carsey, F. D.: Ice motion over Lake Vostok, Antarctica: constraints on inferences regarding the accreted ice, *J. Glaciol.*, 46, 689–694, 2000. 5240
- 15 Le Brocq, A. M., Payne, A. J., and Siegert, M. J.: West Antarctic balance calculations: impact of flux-routing algorithm, smoothing algorithm and topography, *Comput. Geosci.*, 32, 1780–1795, 2006. 5228
- Le Brocq, A. M., Payne, A. J., and Vieli, A.: An improved Antarctic dataset for high resolution numerical ice sheet models (ALBMAP v1), *Earth Syst. Sci. Data*, 2, 247–260, doi:10.5194/essd-2-247-2010, 2010. 5228
- 20 Liboutry, L.: General theory of subglacial cavitation and sliding of temperate glaciers, *J. Glaciol.*, 7, 21–58, 1968. 5227
- Lythe, M. B., Vaughan, D. G., and the BEDMAP Consortium: BEDMAP: a new ice thickness and subglacial topographic model of the Antarctic, *J. Geophys. Res.*, 106, 11335–11351, 2001. 5228
- 25 Maule, C. F., Purucker, M. E., Olsen, N., and Mosegaard, K.: Heat flux anomalies in Antarctica revealed by satellite magnetic data, *Science*, 309, 464–467, 2005. 5236
- Nye, J.: Water at the bed of a glacier, *IASH Publ. 95*, Symposium at Cambridge 1969, Hydrology of Glaciers, 477–489, 1973. 5227
- 30 Pattyn, F.: A new three-dimensional higher-order thermomechanical ice sheet model: basic sensitivity, ice stream development, and ice flow across subglacial lakes, *J. Geophys. Res.*, 108, 1–15, 2003. 5231

A balanced water layer concept

S. Goeller et al.

Title Page

Abstract

Introduction

Conclusions

References

Tables

Figures

◀

▶

◀

▶

Back

Close

Full Screen / Esc

Printer-friendly Version

Interactive Discussion



- Pattyn, F.: Antarctic subglacial conditions inferred from a hybrid ice sheet/ice stream model, *Earth Planet. Sci. Lett.*, 295, 451–461, 2010. 5227, 5228
- Pattyn, F., de Smedt, B., and Souchez, R.: Influence of subglacial Vostok lake on the regional ice dynamics of the Antarctic ice sheet: a model study, *J. Glaciol.*, 50, 583–589, 2004. 5228, 5240
- 5 Quinn, P., Beven, K., Chevallier, P., and Planchon, O.: The prediction of hillslope flow paths for distributed hydrological modelling using digital terrain models, *Hydrol. Process.*, 5, 59–79, 1991. 5228, 5241
- Roethlisberger, H.: Water pressure in intra- and subglacial channels, *J. Glaciol.*, 11, 177–203, 1972. 5227
- 10 Schoof, C.: Ice-sheet acceleration driven by melt supply variability, *Nature*, 468, 803–806, 2010. 5227
- Schoof, C., Hewitt, I. J., and Werder, M. A.: Flotation and free surface flow in a model for subglacial drainage. Part 1. Distributed drainage, *J. Fluid Mech.*, 702, 126–156, 2012. 5227, 5241
- 15 Shapiro, N. M. S. and Ritzwoller, M. H.: Inferring surface heat flux distributions guided by a global seismic model: particular application to Antarctica, *Earth Planet. Sci. Lett.*, 223, 213–224, 2004. 5236
- Siegert, M. J., Carter, S., Tabacco, I. E., Popov, S., and Blankenship, D. D.: A revised inventory of Antarctic subglacial lakes, *Antarct. Sci.*, 17, 453–460, 2005. 5226
- 20 Smith, B. E., Fricker, H. A., Joughin, I. R., and Tulaczyk, S.: An inventory of active subglacial lakes in Antarctica detected by ICESat (2003–2008), *J. Glaciol.*, 55, 573–595, 2009. 5226
- Tarboton, D.: A new method for the determination of flow directions and upslope areas in grid digital elevation models, *Water Resour. Res.*, 33, 309–319, 1997. 5228, 5241
- 25 Thoma, M., Grosfeld, K., Mayer, C., and Pattyn, F.: Interaction between ice sheet dynamics and subglacial lake circulation: a coupled modelling approach, *The Cryosphere*, 4, 1–12, doi:10.5194/tc-4-1-2010, 2010. 5228, 5229, 5240
- Thoma, M., Grosfeld, K., Mayer, C., and Pattyn, F.: Ice-flow sensitivity to boundary processes: a coupled model study in the Vostok Subglacial Lake area, Antarctica, *Ann. Glaciol.*, 53, 173–180, 2012. 5228, 5229, 5240
- 30 Weertman, J.: General theory of water flow at the base of a glacier or ice sheet, *Rev. Geophys. Space Ge.*, 10, 287–333, 1972. 5227

- Wingham, D. J., Siegert, M. J., Shepherd, A., and Muir, A. S.: Rapid discharge connects Antarctic subglacial lakes, *Nature*, 440, 1033–1036, 2006. 5226, 5230, 5241
- Wright, A. and Siegert, M. J.: The identification and physiographical setting of Antarctic subglacial lakes: an update based on recent discoveries, in: *Subglacial Antarctic Aquatic Environments*, *Geophys. Monogr. Ser.*, Vol. 192, AGU, Washington DC, 9–26, 2011. 5226
- 5 Wright, D. G., Siegert, M. J., Le Brocq, A. M., and Gore, D. B.: High sensitivity of subglacial hydrological pathways in Antarctica to small ice-sheet changes, *Geophys. Res. Lett.*, 37, L17504, doi:10.1029/2008GL034937, 2008. 5241

A balanced water layer concept

S. Goeller et al.

Title Page

Abstract

Introduction

Conclusions

References

Tables

Figures

I◀

▶I

◀

▶

Back

Close

Full Screen / Esc

Printer-friendly Version

Interactive Discussion



A balanced water layer concept

S. Goeller et al.

Table 1. Ice volume, change of ice volume compared to the initial state and stored subglacial water volume for all experiments.

| | $V_{\text{ice}} \text{ (km}^3\text{)}$ | $\Delta V_{\text{ice}} \text{ (%)}$ | $V_{\text{water}} \text{ (km}^3\text{)}$ |
|---------------|--|-------------------------------------|--|
| Initial state | 17 051 | | 0 |
| Exp. A | 16 484 | −3.3 | 372 |
| Exp. B | 16 111 | −5.5 | 368 |
| BW A | 16 983 | −0.4 | 0 |
| BW B | 16 666 | −2.3 | 0 |

Title Page

Abstract

Introduction

Conclusions

References

Tables

Figures

◀

▶

◀

▶

Back

Close

Full Screen / Esc

Printer-friendly Version

Interactive Discussion



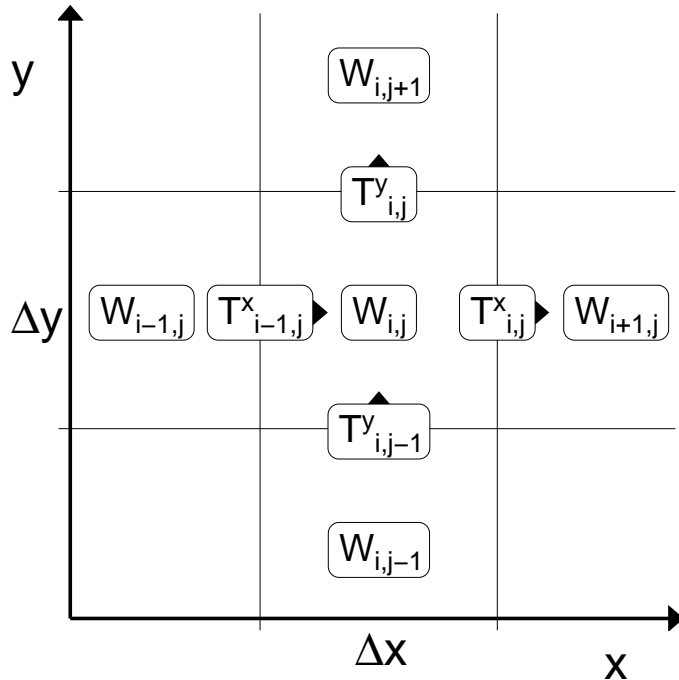


Fig. 1. Notation for staggered Arakawa C-grid: at the grid center: basal water layer thickness $W_{i,j}$, hydraulic potential $P_{i,j}$, normalization $N_{i,j}$, water flux $\phi_{i,j}$ (for coupling to an A-grid ice model), at the grid cell edges: water transport $T_{i,j}^x$ and $T_{i,j}^y$, hydraulic gradients $\partial P_{i,j}/\partial x$ and $\partial P_{i,j}/\partial y$, water flux $\phi_{i,j}^x$ and $\phi_{i,j}^y$ (for coupling to an C-grid ice model).

A balanced water layer concept

S. Goeller et al.

Title Page

Abstract

Introduction

Conclusions

References

Tables

Figures

◀

▶

◀

▶

Back

Close

Full Screen / Esc

Printer-friendly Version

Interactive Discussion



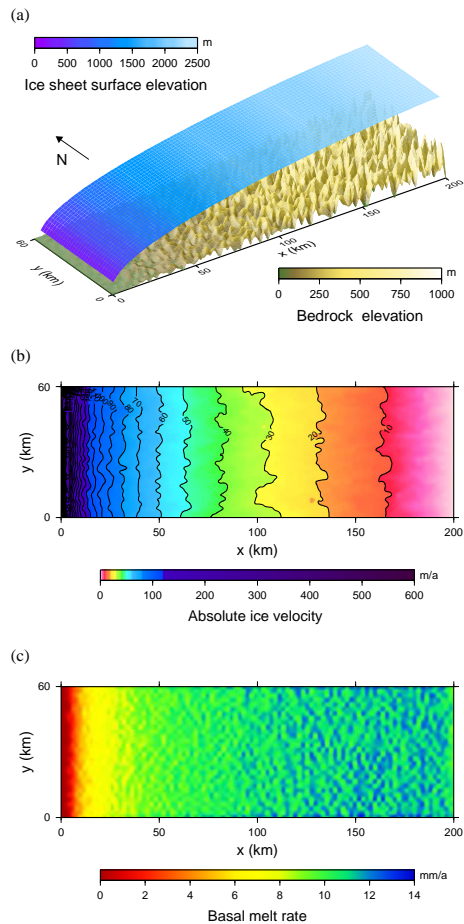


Fig. 2. Initial state: **(a)** model domain with mountainous bedrock and steady-state ice sheet topography, **(b)** absolute ice velocities and **(c)** basal melt rates.

A balanced water layer concept

S. Goeller et al.

Title Page

Abstract Introduction

Conclusions References

Tables Figures

◀ ▶

◀ ▶

Back Close

Full Screen / Esc

Printer-friendly Version

Interactive Discussion



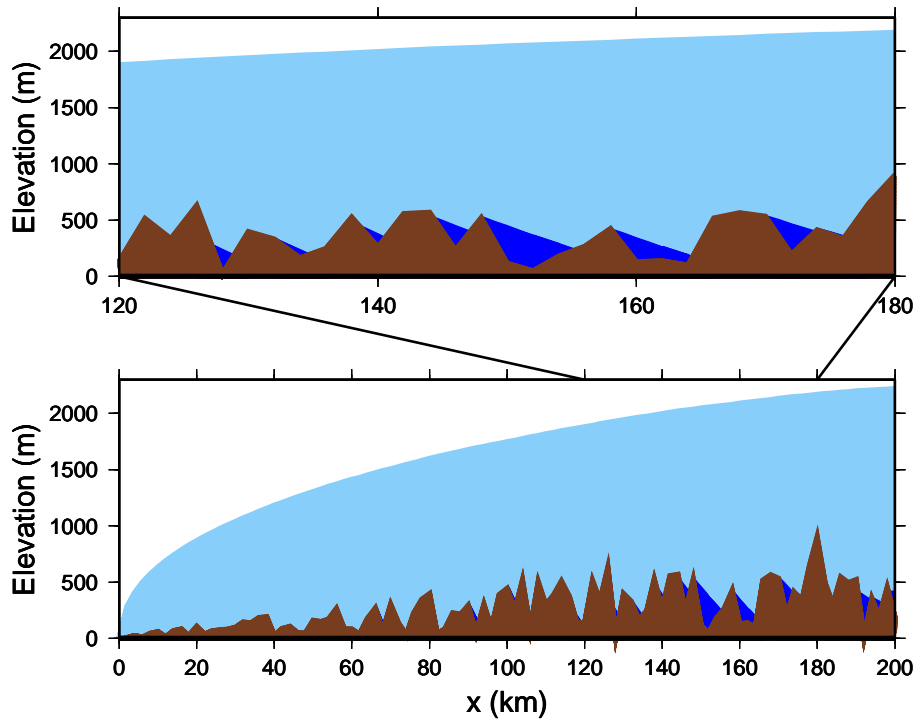


Fig. 3. Exp. A: Profile of the ice sheet at $y = 22$ km, showing several subglacial lakes and their inclined surfaces due to the ice sheet surface gradients, similar to observed profiles in Antarctica (Bell et al., 2011).

A balanced water layer concept

S. Goeller et al.

| | |
|--|------------------------------|
| Title Page | |
| Abstract | Introduction |
| Conclusions | References |
| Tables | Figures |
| ◀ | ▶ |
| ◀ | ▶ |
| Back | Close |
| Full Screen / Esc | |
| Printer-friendly Version | |
| Interactive Discussion | |



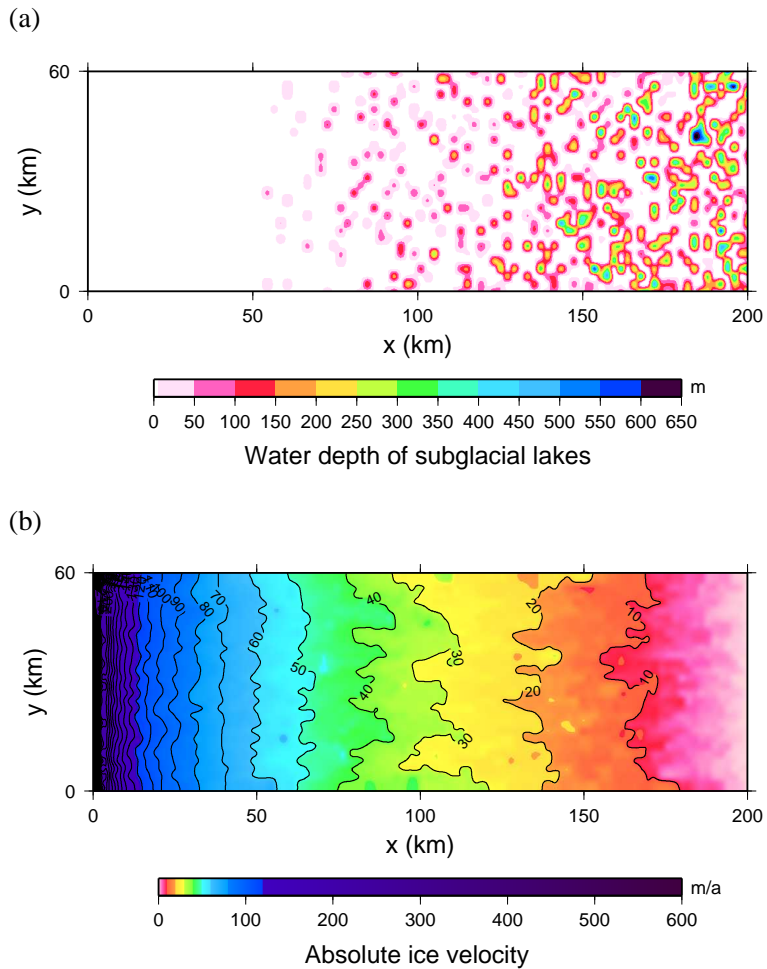


Fig. 4. Exp. A: **(a)** water depths of subglacial lakes and **(b)** absolute ice velocities.

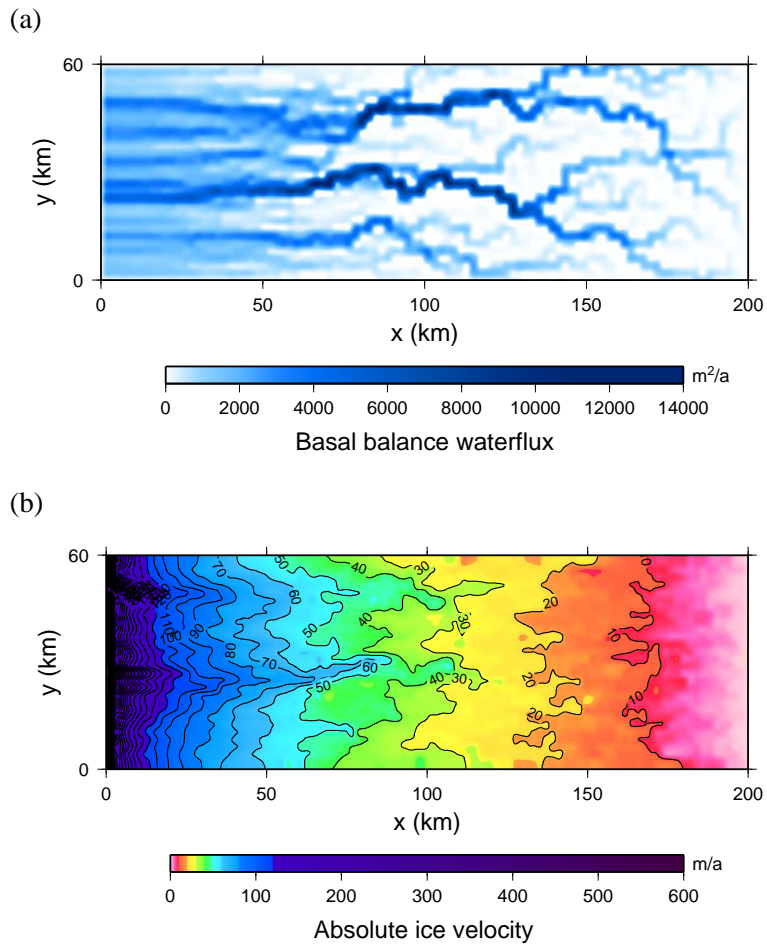


Fig. 5. Exp. B: (a) basal balance water flux and (b) absolute ice velocities.

A balanced water layer concept

S. Goeller et al.

Title Page

Abstract

Introduction

Conclusions

References

Tables

Figures

◀

▶

◀

▶

Back

Close

Full Screen / Esc

Printer-friendly Version

Interactive Discussion



A balanced water layer concept

S. Goeller et al.

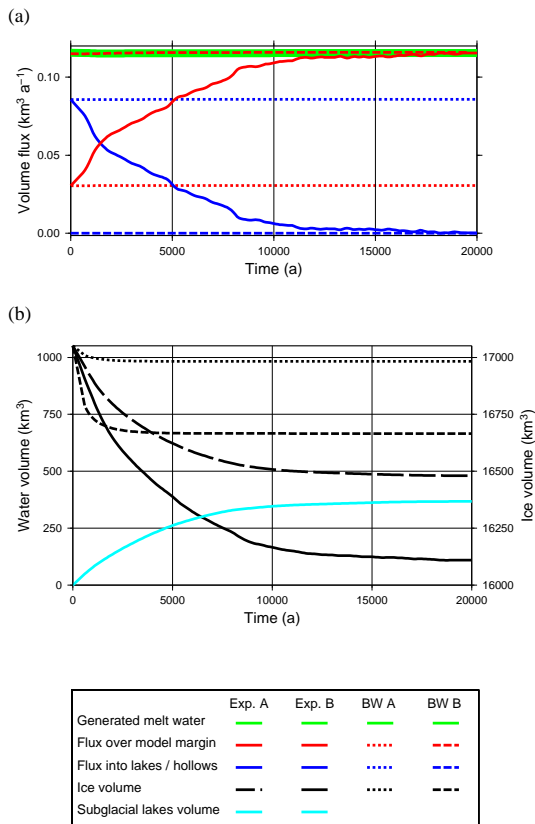


Fig. 6. (a) Subglacial water balance and (b) ice and subglacial lake volume for different basal hydrology models. (Experiments with very similar results share one line style.)

Title Page

Abstract Introduction

Conclusions References

Tables Figures

◀ ▶

◀ ▶

Back Close

Full Screen / Esc

Printer-friendly Version

Interactive Discussion



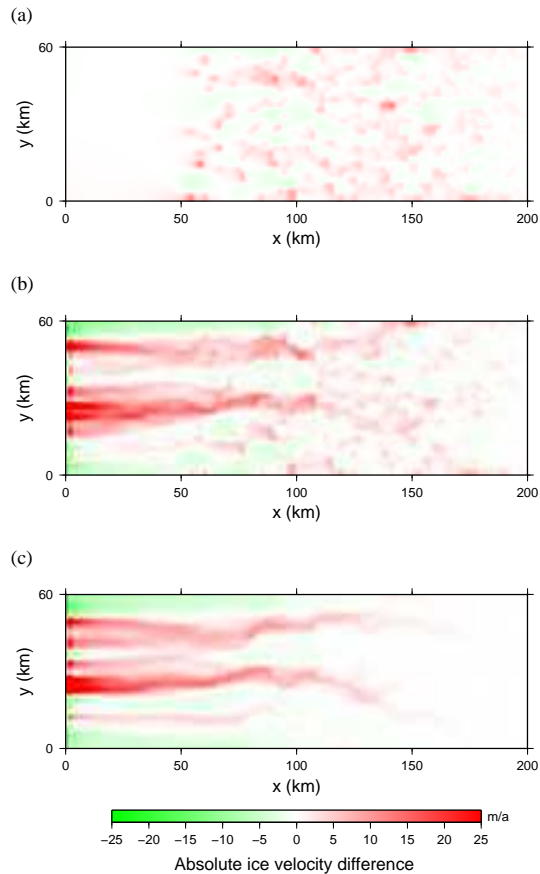


Fig. 7. Absolute ice velocity variations of **(a)** Exp. A, **(b)** Exp. B and **(c)** BW B compared to the initial state.

A balanced water layer concept

S. Goeller et al.

Title Page

Abstract Introduction

Conclusions References

Tables Figures

◀ ▶

◀ ▶

Back Close

Full Screen / Esc

Printer-friendly Version

Interactive Discussion

